# Combined UV/Vis and NMR spectroscopy allows for *operando* reaction monitoring: the case of guaiazulene and 2,4-dinitrobenzaldehyde Supporting Information

Kilian Heckenberger[a] and Christina M. Thiele*[a]

## Table of Contents

## 1. General Information

**NMR spectroscopy:**
All $^{1}H$, $^{13}C$ and $^{31}P$ NMR experiments were carried out on a Bruker Avance III spectrometer with 600.3 MHz proton frequency, equipped with a 5 mm Triple Resonance Broadband Probe (TBI) ($^{1}H/^{31}P$-BB/$^{2}H$) with z-gradient and a BCU-extreme for temperature regulation.
$^{19}F$ NMR experiments were carried out on a Bruker Avance III HD spectrometer with 700.1 MHz proton frequency, equipped with a QCI cryoprobe ($^{1}H/^{19}F$-$^{31}P/^{13}C/^{15}N/^{2}H$) with z-gradient and a BCU-II.
Unless stated otherwise, NMR spectra are recorded at 300 K, and processed with exponential line broadening of 0.3 Hz and zero-filling with a factor of 2. NMR chemical shifts are referenced using the residual solvent signal. NMR spectra are processed using TopSpin (version 3.5 pl 7).

For details on spectra acquisition and processing see sections SI-3 and SI-4.

**UV/Vis (conventional):**
A conventional UV/Vis spectrometer (JASCO V-630 spectrophotometer) with 1 mm quartz cuvettes (manufacturer: Starna, type: 21, material: Q)) was used for acquisition of UV/Vis absorption spectra. UV/Vis spectra were recorded in a wavelength range from 300 to 800 nm with a 0.5 nm interval size, without spectra accumulation.

**UV/Vis (combined monitoring):**
The UV/Vis setup for combined monitoring was adapted from [1] with minor adaptations. These are described in section SI-2. As the light source, we used an AvaLight-DH-S-BAL by Avantes. As the UV/Vis spectrometer, we used StarLine, AvaSpec-3648 with replaceable slit by Avantes. The slit width used for all measurements is 200 μm.

For details on spectra acquisition and processing see sections SI-3 and SI-5.

**Chemicals:**
Chemicals were obtained from Sigma Aldrich and used without further purification. Deuterated solvents from sealed ampules were used. The degree of deuteration of the deuterated solvents used is ≥99.9% for acetone-$d_6$ and ≥99.5% for tetrahydrofuran-$d_8$ (THF-$d_8$)

**Mass spectrometry:**
HR-ESI mass spectra for compound characterisation were acquired on a Bruker Impact II instrument, using positive and negative ion mode.

**Infrared spectroscopy:**
Infrared spectra were acquired on a Bruker ALPHA FT-IR instrument equipped with a Platinum-ATR unit.

## 2. Adapted dip-probe setup for combined *operando* UV/Vis and NMR spectroscopy

For combined UV/Vis and NMR monitoring we use a slightly altered version of the dip-probe setup described in detail in our earlier publication [1] (therein: supporting information, p. 2-4).

For the non-rapid injection setup used in this work, we modified the setup as follows:

- The illumination fibre (dip_a) is not used.
- Instead of the large volume insert (dip_h) we use an insert with smaller volume, since it only needs to accommodate the UV/Vis fibre bundle (dip_b). We use the insert WGS-5BL by Wilmad-LabGlass (8 inch x (O.D. < 4.2 mm); stem O.D. 2.0 mm).

## 3. Acquiring spectra with *operando* monitoring

For preparing *operando* measurements, stock solutions of the reagents (guaiazulene **1**, 2,4-dinitrobenzaldehyde **2**) are prepared in (deuterated) solvent (THF or acetone), in order to reduce weighing errors. These solutions are used within a few days and stored at 0 °C, as solvent evaporation can significantly alter the concentrations. Concentrated $HPF_6$ is diluted with the respective solvent prior to use.

Usual amounts, used for a reactant ratio of around 1:1.5 (guaiazulene:dinitrobenzaldehyde), are approximately:

- 1.4 to 1.8 mg of guaiazulene **1** in 2.5 to 3.5 mL of solvent.
- 1.6 to 2.5 mg of 2,4-dinitrobenzaldehyde **2** in 0.4 to 0.6 mL of solvent.
- 20 μL of conc. $HPF_6$ are dissolved in 60 μL of solvent. The amount is transferred via Eppendorf pipette to either reactant solution.

Exact amounts are given in table SI-1.

**Table SI-1** Overview on sample preparation details. Samples used for main text figures are marked as bold and underlined.

| Sample no. | *c*(1) / mmol $L^{-1}$ | *c*(2) / mmol $L^{-1}$ | *c*($HPF_6$) / mmol $L^{-1}$ | solvent | Referenced in … | Sample type |
|---|---|---|---|---|---|---|
| **kh03-050** | 129 | 196 | 534 | diethyl ether | section SI-7 | Synthesis of **3** |
| **kh03-051-A** | -- | -- | -- | acetone-$d_0$ | figure SI-6 | UV/Vis characterisation of **3** |
| **kh03-052** | -- | -- | -- | acetone-$d_6$ | section SI-7 | NMR characterisation of **3** |
| **kh03-039-B** | 2.1 | 3.4 | 54.2 | THF-$d_8$ | figure SI-7 | Identification of **4** with temperature variation |
| **kh03-039-C** | 2.1 | 3.4 | 54.2 | THF-$d_8$ | section SI-8 | Identification of **4** (from monitoring) |
| **kh03-041** | 63.6 | -- | 205 | THF-$d_8$ | section SI-9 | Identification of **1+H$^+$** |
| **kh03-002** | 420 | -- | -- | THF-$d_8$ | section SI-6 | NMR characterisation of **1** |
| **kh03-014** | -- | 12.4 | -- | THF-$d_8$ | section SI-6 | NMR characterisation of **2** |
| **kh03-058** | -- | 68.7 | -- | THF-$d_8$ | section SI-6 | NMR characterisation of **2** |
| **kh03-045-A** | 9.99 | -- | -- | THF-$d_0$ | figure SI-5 | UV/Vis characterisation of **1** |
| | | | | | | |
| **kh03-035-C** | 2.5 | 3.4 | 53.8 | THF-$d_8$ | **figure 2**<br>figure SI-2<br>figure SI-4 | *Operando* UV/Vis monitoring |
| | | | | | | |
| **kh03-053-B** | 2.1 | 3.0 | 108 | THF-$d_8$ | **figure 3c**<br>figure SI-8 | *Operando* NMR monitoring |
| **kh03-043-A** | 2.1 | 3.1 | 53.8 | THF-$d_8$ | **figures 3a, b**<br>figure SI-8 | *Operando* NMR monitoring |
| **kh03-054-B** | 2.1 | 3.0 | 27.1 | THF-$d_8$ | figure SI-8 | *Operando* NMR monitoring |
| **kh03-053-A** | 2.1 | 3.0 | 20.3 | THF-$d_8$ | **figure 3d**<br>figure SI-8 | *Operando* NMR monitoring |
| **kh03-040-A** | 8.6 | 3.1 | 54.2 | THF-$d_8$ | figure SI-9 | *Operando* NMR monitoring |
| | | | | | | |
| **kh03-039-E** | 2.1 | 3.5 | 54.7 | THF-$d_8$ | **figure 1**<br>**figure 4**<br>figure SI-1<br>figure SI-2<br>figure SI-3 | Combined o*perando* NMR and UV/Vis monitoring |

***Operando* UV/Vis monitoring (conventional):**
200 µL of the guaiazulene solution are loaded into a cuvette (path length 1 mm). A spectrum is recorded, serving as the $t_0$ data point. Then, 50 µL of the second reactant solution are mixed with the $HPF_6$ solution and added to the same cuvette. The solution is mixed by shaking. The cuvette is quickly transferred back to the UV/Vis spectrometer. The monitoring is conducted by measuring UV/Vis spectra in the range from 250 to 800 nm with a repetition time of $t_{rep}$ = 40 s. The usual dead time is around 40 s.

***Operando* NMR monitoring (conventional):**
500 µL of the guaiazulene solution (in deuterated solvent) is mixed with the $HPF_6$ solution and loaded into an NMR tube (O.D. 5 mm). A spectrum is recorded, serving as the $t_0$ data point. Then, 100 µL of the second reactant solution are added to the same NMR tube. The solution is mixed by shaking. The NMR tube is quickly transferred back to the NMR spectrometer. Measuring can be started immediately, as the instrument is already set up from the $t_0$ measurement. The monitoring is conducted by measuring NMR spectra with a repetition time of $t_{rep}$ = 60 s. The usual dead time is around 60 s.

**Combined *operando* NMR and UV/Vis monitoring:**
For UV/Vis reference, a sample of pure solvent is measured. For that, a thin-walled NMR tube (O.D. 5 mm) is loaded with solvent. The combined setup is assembled according to [1]. The NMR tube is adjusted so that the insert has a distance of around 1 mm to the PTFE mirror. A dark and reference spectrum are measured. Then, only the NMR tube is disassembled from the setup, leaving the rest intact for quick reassembly.
250 µL of the guaiazulene solution (in deuterated solvent) are loaded into a separate thin-walled NMR tube. The combined setup is assembled and an NMR and a UV/Vis spectrum are recorded, serving as the $t_0$ data point. If necessary, the UV/Vis pathlength can be adjusted according to the measured UV/Vis intensity. In case of readjustment, reference and dark spectra can be re-measured after the monitoring. Then, only the NMR tube is disassembled from the setup.
50 µL of the second reactant solution are mixed with the $HPF_6$ solution and added to the same NMR tube. The solution is mixed by shaking. The combined setup is quickly reassembled, adjusting the UV/Vis pathlength to the value used before. The setup is quickly transferred back to the NMR spectrometer and NMR and UV/Vis measurements are started immediately. The monitoring is conducted by measuring NMR spectra and UV/Vis spectra quickly after each other, with a repetition time of $t_{rep}$ = 60 s. The usual dead time is around 120 s.

## 4. Processing NMR spectra from *operando* monitoring

**Processing NMR spectra:**
NMR spectra from reaction monitoring are processed in a serial manner, using automated phase and baseline correction. Serial integration is performed by referencing to one of the methyl signals of guaiazulene in the first spectrum. We use this data point from reaction monitoring (usually $t$ = 60 s or 120 s), instead of the spectrum at $t_0$. We do this, because spectra recorded on the ongoing reaction are more comparable with each other (due to change in sample volume and susceptibility, as well as changes introduced by reassembly) and the reaction is slow enough, that it has not progressed significantly within 60 to 120 s.

In cases of high $HPF_6$ concentration, protonated guaiazulene **1+H⁺** is detected in the NMR spectra. For sake of simplification, the total amount of guaiazulene is considered to be the sum of **1** and **1+H⁺**. The NMR identification of **1+H⁺** is described in section SI-9.

The resulting integrals are normalised according to the number of chemically equivalent protons. The integral-time courses for all protons of a species are compared and the time course with the least noise and overlap is chosen for display. In case where signals of two known species overlap, the integral for one of the species can be calculated by subtracting the normalised integral of the other species (details see below).

For the combined monitoring approaches, automatic baseline correction for the full spectrum is made difficult by a background polymer signal, caused by the glue in the tip of the glass fibre bundle. Therefore, automatic baseline correction is performed only to the spectral regions of interest.

The obtained series of NMR spectra from combined NMR-UV/Vis monitoring, including a highlight of the signals used for integration, is depicted in Figure SI-1.

**Normalisation of integrals:**
The NMR signals are integrated for all spectra of a monitoring run. Integral values are obtained using serial integration, where the signal of the $CH_3$ group of **1** at 2.82 ppm in the first spectrum is set as the reference point.

Species **1**: The plot is given as the sum of species **1** and **1+H⁺**. For monitoring runs where no **1+H⁺** is observed, only the integral of **1** is taken. This is the case for combined NMR-UV/Vis monitoring (Figure 4) and NMR monitoring at c($HPF_6$) = 20 mM (Figure 2c and Figure SI-8).

The integral of **1** is determined from the $CH_3$ group signal at 2.82 ppm.
$I_{norm}$(**1**) = $I$(2.82 ppm)/3

The integral of **1+H⁺** is determined from the $CH_2$ group signal at 4.15 ppm (H1, see section SI-9; used for c($HPF_6$) = 27 mM and 54 mM) or the $CH_3$ group signal at 2.46 ppm (H11; used for c($HPF_6$) = 108 mM).

In the former case, the normalised integral is calculated as follows:
$I_{norm}$(**1+H⁺**) = $I$(4.15 ppm)/2

The latter signal (2.46 ppm) is used due to overlap of the 4.15 ppm signal with a signal of a standard substance used only in this monitoring run (c($HPF_6$) = 108 mM). However, the signal of **1+H⁺** at 2.46 ppm overlaps with a $CH_3$ group signal of **4**. Therefore, in this case the normalised integrals of **1+H⁺** is determined as follows:

$I$(2.46 ppm) = 3*$I_{norm}$(**1+H⁺**) + 3*$I_{norm}$(**4**)
→ $I_{norm}$(**1+H⁺**) = $I$(2.46 ppm)/3 - $I_{norm}$(**4**)

$I_{norm}$(**4**) = $I$(2.94 ppm)/6 (see below)
→ $I_{norm}$(**1+H⁺**) = $I$(2.46 ppm)/3 - $I$(2.94 ppm)/6

Species **3**: The integral of **3** is determined from the signal of the two (isopropyl) $CH_3$ groups at 1.54 ppm.
$I_{norm}$(**3**) = $I$(1.54 ppm)/6

Species **4**: The integral of **4** is determined from the two signals of the two $CH_3$ groups at 2.94 ppm. At 300 K the signals are not separated, which we attribute to partially hindered intramolecular rotation. Therefore, the integration range is chosen to include both signals.
$I_{norm}$(**4**) = $I$(2.94 ppm)/6

For a uniform display of the results, all integrals within a monitoring run are rescaled by the same constant $C$ so that the sum of the normalised intensities of **1** and **1+H**$^+$ is 1 at the first time point of recording.

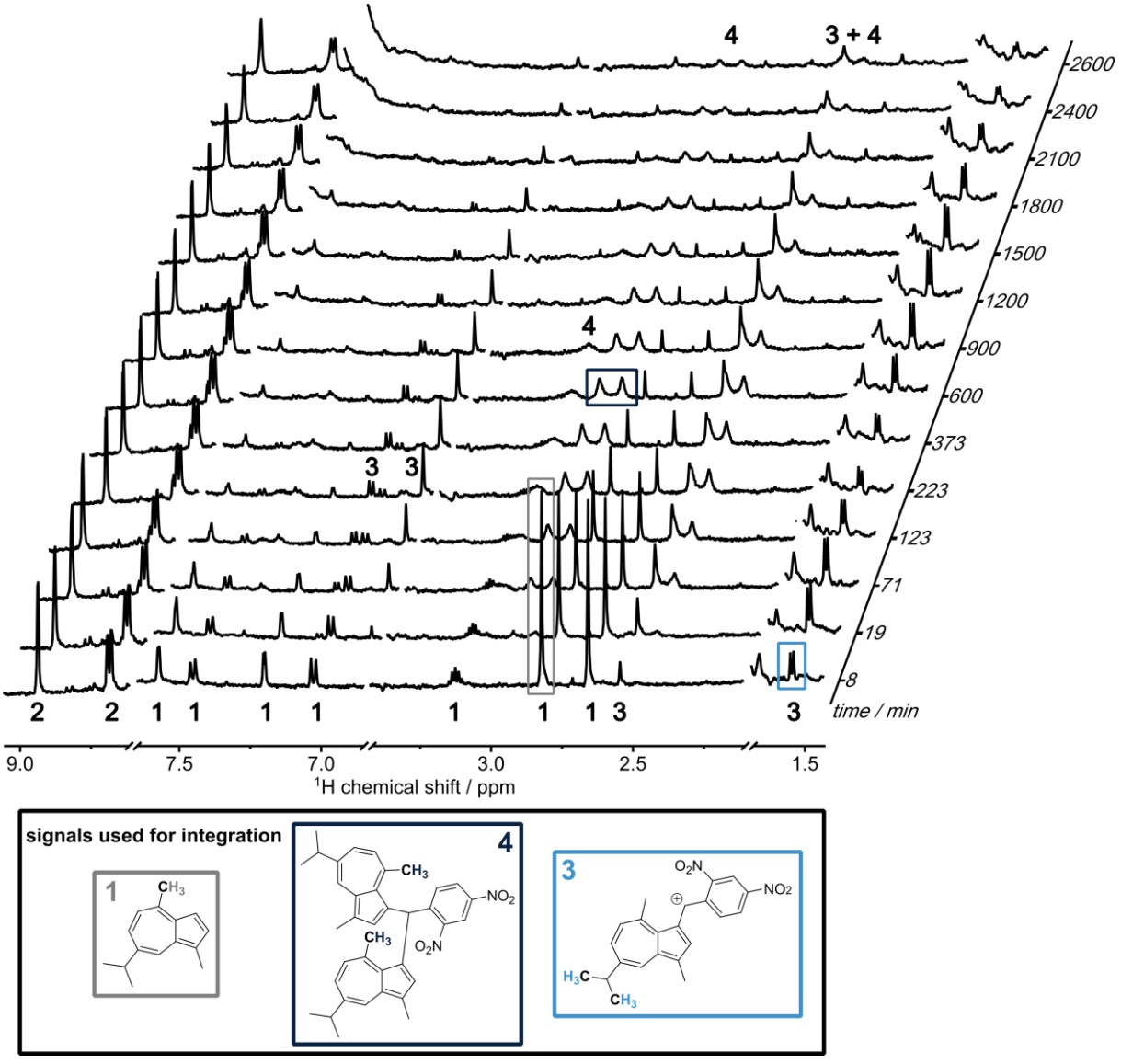


**Figure SI-1** Series of NMR spectra from reaction monitoring of the reaction between guaiazulene **1** and 2,4-dinitrobenzaldehyde **2**, using combined NMR-UV/Vis monitoring. Sample no. kh03-039-E, **1**:**2**:$HPF_6$ = 2.1:3.5:54.7 mmol/L). The signals of species **1** to **4** are marked using the according numbers. The signals used for integration are marked by a coloured frame (grey: **1**, light blue: **3**, dark blue: **4**). The corresponding positions in the molecule are marked in the structures below the spectra. For visual clarity, spectra are cut to show representative regions (signals of residual solvent and $H_2O$ are omitted) and not all spectra are shown.

## 5. Processing UV/Vis spectra from *operando* monitoring

**Processing UV/Vis spectra:**
For conventional UV/Vis spectroscopy, the obtained UV/Vis spectra/absorption values are used as obtained from the JASCO instrument software.

For UV/Vis spectra obtained with the combined setup, processing is done as explained in [1], section SI 2.2.3. Of the two options for smoothing the spectra, we decided on using linear smoothing with a 6 pt window.

**Baseline correction:**
Furthermore, baseline correction needs to be applied. This is best demonstrated by comparing the spectra series from conventional monitoring (fig. SI-2 left) to that of combined monitoring (fig. SI-2 right). In conventional monitoring, the absorption at 800 nm is close to 0. This is clearly not the case for combined monitoring. Therefore, a correction has to be applied in order to correct for instrumental effects. The exact cause of these effects is unknown. However, we suspect that over time, decomposition products of unknown identity settle on the PTFE mirror, lowering reflectance.

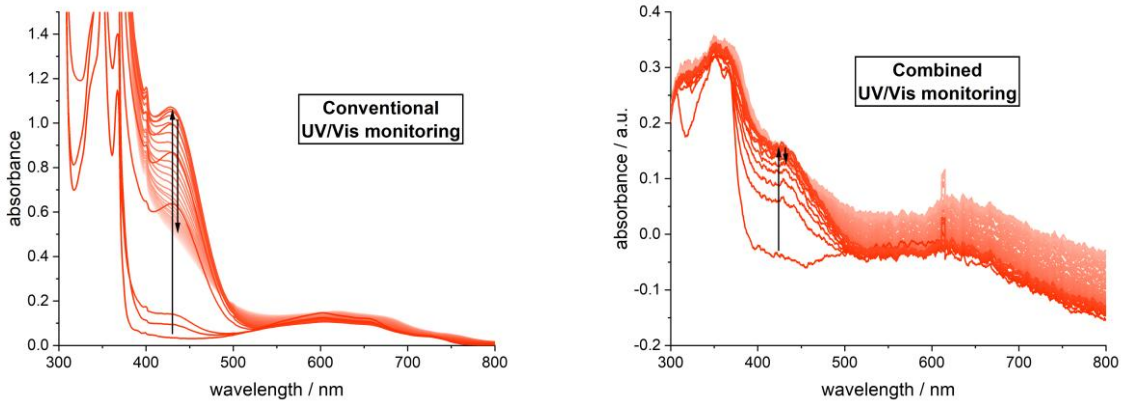


**Figure SI-2** Series of UV/Vis spectra from reaction monitoring of the reaction between guaiazulene **1** and 2,4-dinitrobenzaldehyde **2**. Left: Conventional *operando* UV/Vis monitoring (sample no. kh03-035-C, **1**:**2**:$HPF_6$ = 2.5:3.4:53.8 mmol/L). Right: UV/Vis spectra from combined *operando* NMR and UV/Vis monitoring (sample no. kh03-039-E, **1**:**2**:$HPF_6$ = 2.1:3.5:54.7 mmol/L). Time is indicated by the colour: dark red (reaction start) to white.

Similar to the baseline correction employed in [1], a point in the spectrum is chosen, where no absorption should occur throughout the reaction. In our case, we choose the data point at 800 nm, as there should be (almost) no absorption, according the conventionally recorded UV/Vis spectra (fig. SI-2 left). The spectra series from combined monitoring before and after baseline correction are displayed in figure SI-3.

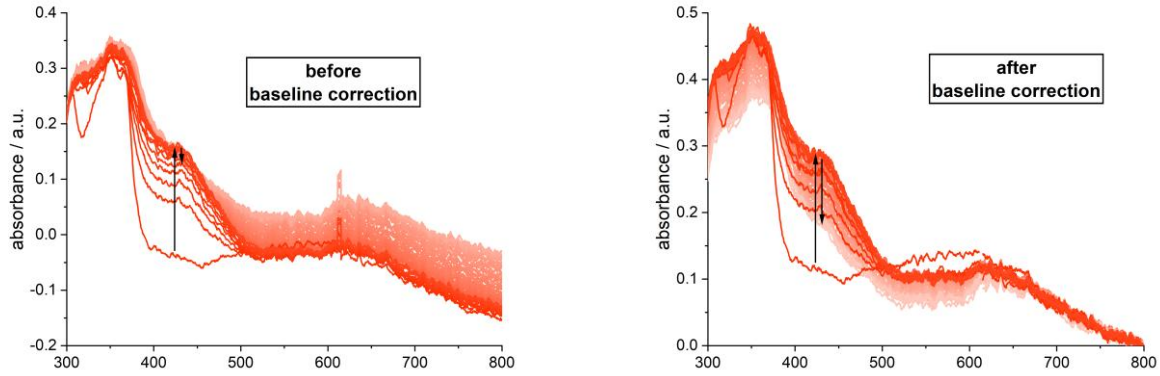


**Figure SI-3** Series of UV/Vis spectra obtained from combined *operando* NMR and UV/Vis monitoring (sample no. kh03-039-E, **1**:**2**:$HPF_6$ = 2.1:3.5:54.7 mmol/L). Left: Before applying baseline correction. Right: After applying baseline correction, where all spectra were set to an absorbance value of 0 at 800 nm. Time is indicated by the colour: dark red (reaction start) to white.

**Signal overlap in UV/Vis spectra:**

In the early stage of the reaction (here: up to 750 min), the UV/Vis band of species **3** at $\lambda_{max}$ = 430 nm is clearly visible (fig. SI-4 left). At the later stages of the reaction (here: starting at 750 nm), no characteristic band at $\lambda_{max}$ = 430 nm is visible (fig. SI-4 right). We assume that this is due to signal overlap from unidentified species at lower wavelengths, obscuring the observation of a characteristic peak. In this case, species **3** would still contribute to the total spectrum, which is supported by the combined measurements (fig. 4 in the main text), since a second concentration maximum of **3** is also observed with NMR spectroscopy. While the spectra can be evaluated for a qualitative time course analysis, determination of concentration is made difficult by signal overlap, especially for the later stages of the reaction.

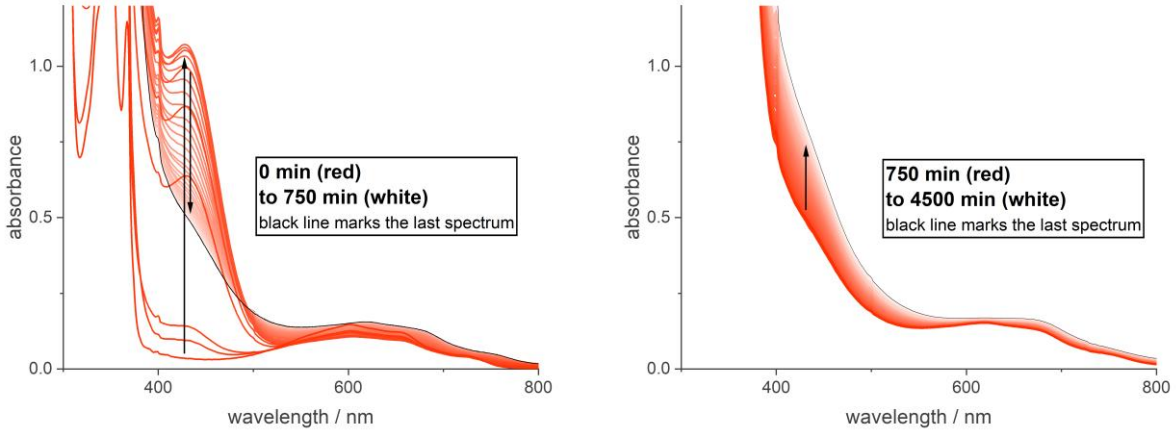


**Figure SI-4** Series of UV/Vis obtained from conventional *operando* UV/Vis monitoring (sample no. kh03-035-C, **1**:**2**:$HPF_6$ = 2.5:3.4:53.8 mmol/L). Left: Spectra from 0 to 750 minutes. Right: Spectra from 750 to 4500 minutes.

## 6. Spectral data of 1 and 2

The spectral data and signal assignment for guaiazulene is in accordance with literature.[2]

**$^1$H-NMR of 1** (THF-$d_8$, 600 MHz, 300 K): $\delta$/ppm = 8.26 (d, $^4J_{H4\text{-}H6}$ = 1.7 Hz, 1H$_4$), 7.62 (d, $^3J_{H2\text{-}H1}$ = 3.6 Hz, 1H$_2$), 7.44 (dd, $^3J_{H6\text{-}H7}$ = 10.7 Hz, $^4J_{H6\text{-}H4}$ = 1.8 Hz, 1H$_6$), 7.24 (d, $^3J_{H1\text{-}H2}$ = 3.7 Hz, 1H$_1$), 7.02 (d, $^3J_{H7\text{-}H6}$ = 10.6 Hz, 1H$_7$), 3.12 (sept, $^3J_{H12\text{-}H13}$ = 6.9 Hz, 1H$_{12}$), 2.83 (s, 3H$_{14}$), 2.70 (s, 3H$_{11}$), 1.41 (d, $^3J_{H13\text{-}H12}$ = 6.9 Hz, 6H$_{13}$).

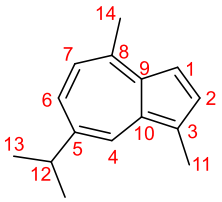


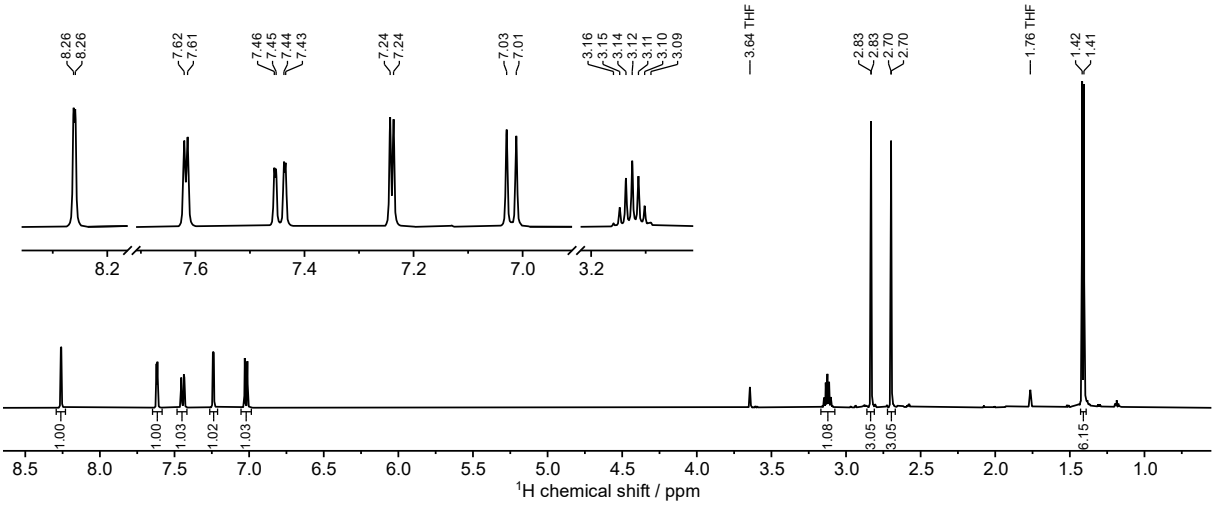


**$^1$H NMR of 2** (THF-$d_8$, 600 MHz, 300 K): $\delta$/ppm = 10.39 (d, $^5J_{H1\text{-}H6}$ = 0.7 Hz, 1H$_1$), 8.95 (d, $^4J_{H4\text{-}H6}$ = 2.2 Hz, 1H$_4$), 8.69 (ddd, $^3J_{H6\text{-}H7}$ = 8.4 Hz, $^4J_{H6\text{-}H4}$ = 2.2 Hz, $^5J_{H6\text{-}H1}$ = 0.7 Hz, 1H$_6$), 8.17 (d, $^4J_{H7\text{-}H6}$ = 8.4 Hz, 1H$_7$).

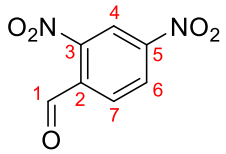


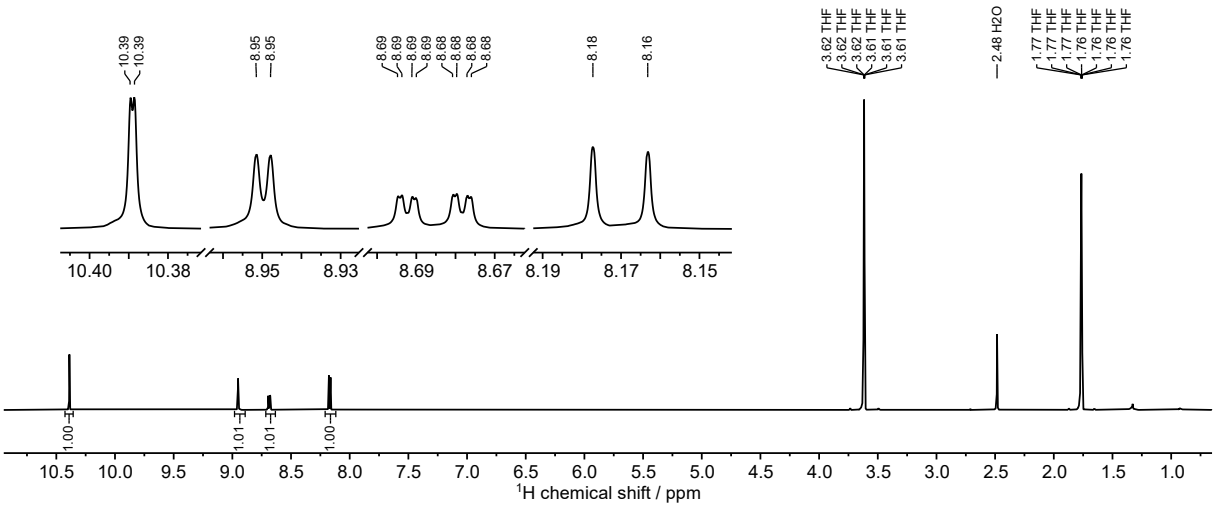

**UV/Vis spectrum of 1:**

39.6 mg (199.7 µmol) of **1** were dissolved in 20 mL THF (9.985 mmol/L) (for the UV/Vis spectrum see figure SI-5 left). From that, solutions with concentrations of 4.993, 1.997, 0.999, 0.499 mmol/L were created by dilution. The absorbance is plotted against the concentration, allowing for a linear fit (fig. SI-5 right) according to the LAMBERT BEER equation ($\varepsilon$: extinction coefficient in L mmol$^{-1}$ mm$^{-1}$, *A*: absorbance in a.u., *c*: concentration in mmol L$^{-1}$, *d*: path length in mm).

$$\varepsilon = \frac{\partial \mathrm{A}}{\partial \mathrm{c}} \cdot \frac{1}{\mathrm{d}}$$

The resulting value for the extinction coefficient at 602 nm is $\varepsilon$ = 0.0445 L mmol$^{-1}$ mm$^{-1}$.

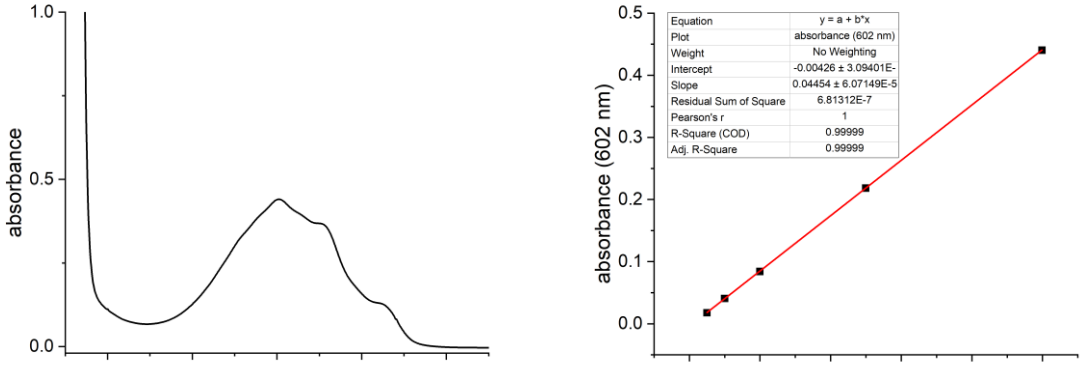


**Figure SI-5** Left: UV/Vis spectrum of species **1**. Right: Linear fit for the determination of the extinction coefficient of species **1**.

## 7. Synthesis and characterisation of (2,4-dinitrophenyl)(5-isopropyl-3,8-dimethylazulen-1-yl)methylium hexafluorophosphate (3)

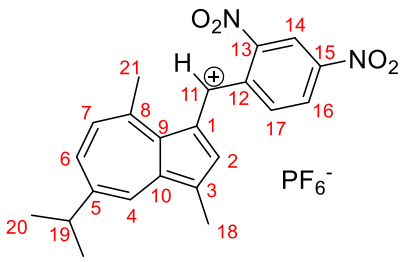


The synthesis of (2,4-dinitrophenyl)(5-isopropyl-3,8-dimethylazulen-1-yl)methylium hexafluorophosphate (**3**) is conducted according to the literature procedure for other cationic aryl-azulenyl-methylium species.[3]

Synthesis (sample no. kh03-050): 256 mg (1.29 mmol, 1.0 eq.) of guaiazulene (**1**) and 385 mg (1.96 mol, 1.5 eq.) of 2,4-dinitrobenzyldehyde (**2**) are dissolved in 10 mL of diethyl ether (DE), giving a dark blue solution. With stirring, the reaction is started by adding 800 µL of concentrated hexafluorophosphoric acid (55% in $H_2O$) (amounts to 5.34 mol, 4.1 eq. of pure $HPF_6$). The reaction quickly turns from blue to green to dark yellow. The reaction mixture is stirred for 150 minutes at room temperature. During this time, a dark green residue precipitates from the dark yellow reaction solution.

Workup: To the biphasic mixture obtained in the previous step, dichloromethane (DCM) is added until all of the green residue is dissolved (around 50 mL). The solution is washed with 10 mL of water. The organic phase is evaporated with a rotavap to give dark green crude product. The dark green residue is dissolved in as little as possible DCM (around 3 mL) and precipitated by adding the resulting solution to toluene (50 mL). The dark green residue is filtered off and washed with 3x10 mL of toluene. In order to remove remaining toluene, the resulting crude product is dissolved in as little as possible DCM (around 2.5 mL), and the solution precipitated by adding it to diethyl ether. The precipitate is washed with 3 x 10 mL diethyl ether. The resulting dark green crude product is dried at 40 °C in vacuum with stirring over 72 h. The final product is obtained as a dark green powder with a yield of 469 mg (0.90 mmol, 70 %) and a purity of over 95 mol% ($^1$H-NMR).

**$^1$H-NMR** (acetone-$d_6$, 600 MHz, 300 K): δ/ppm = 9.38 (s, 1$H_{11}$), 9.12 (d, $^4J_{H14\text{-}H16}$ = 2.3 Hz, 1$H_{14}$), 8.96 (d, $^3J_{H7\text{-}H6}$ = 11.3 Hz, 1$H_7$), 8.94 (d, $^4J_{H4\text{-}H6}$ = 2.2 Hz, 1$H_4$), 8.83 (dd, $^3J_{H6\text{-}H7}$ = 11.4, $^4J_{H6\text{-}H4}$ = 2.3 Hz, 1$H_6$), 8.81 (dd, $^3J_{H16\text{-}H17}$ = 8.2, $^4J_{H16\text{-}H14}$ = 2.2 Hz, 1$H_{16}$), 8.14 (d, $^3J_{H17\text{-}H16}$ = 8.4 Hz, 1$H_{17}$), 7.76 (s, 1$H_2$), 3.72 (sept, $^3J_{H19\text{-}H20}$ = 7.0 Hz, 1$H_{19}$), 3.58 (s, 3$H_{21}$), 2.60 (s, 3$H_{18}$), 1.57 (d, $^3J_{H20\text{-}H19}$ = 6.9 Hz, 6$H_{20}$).

**$^{13}$C-NMR** (acetone-$d_6$, 150 MHz, 300 K): δ/ppm = 174.1 (1$C_5$), 163.0 (1$C_3$), 158.3 (1$C_8$), 152.4 (1$C_9$), 152.2 (1$C_7$), 148.7 (1$C_{15}$), 148.4 (1$C_{13}$), 147.0 (1$C_{10}$), 145.4 (1$C_6$), 143.4 (1$C_{11}$), 141.5 (1$C_1$), 139.8 (1$C_4$), 139.2 (1$C_2$), 137.3 (1$C_{12}$), 135.5 (1$C_{17}$), 128.4 (1$C_{16}$), 120.5 (1$C_{14}$), 39.7 (1$C_{19}$), 28.1 (1$C_{21}$), 22.8 (2$C_{20}$), 12.9 (1$C_{18}$).

**$^{31}$P-NMR** (acetone-$d_6$, 245 MHz, 300 K): δ/ppm = -144.3 (sept, $^1J_{PF}$ = 707.9 Hz).

**$^{19}$F-NMR** (acetone-$d_6$, 659 MHz, 300 K): δ/ppm = -72.6 (d, $^1J_{PF}$ = 708.1 Hz).

The $^1$H and $^{13}$C assignment was carried out using HSQC, HMBC and ROESY 2D NMR spectra. The $^{19}$F and $^{31}$P NMR spectra are in agreement with literature data on $PF_6^-$ anions.[4] $^{31}$P spectra were recorded over the whole range of usual chemical shifts (200 to -350 ppm) in order to rule out other phosphorus containing species. Since no other species are observed, the additional signal in the ESI MS spectrum (negative ion mode) at $m/z$ = 313 u is attributed to a cluster species formed in the MS measurement. For the $^{31}$P NMR measurements, multiple spectra were recorded at different offsets to make sure that the whole spectral range is excited.

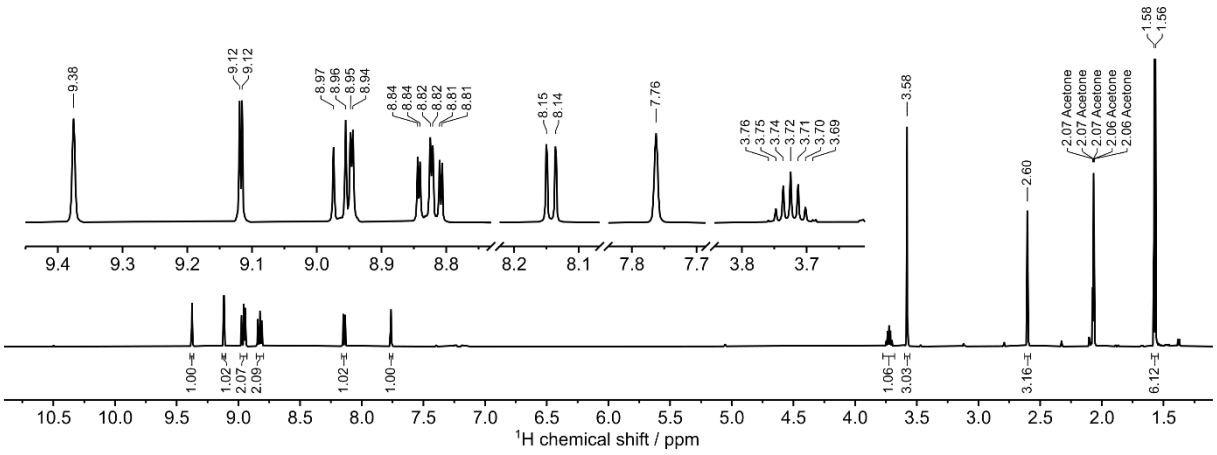
9.38
9.12
9.12
8.97
8.96
8.95
8.94
8.84
8.84
8.82
8.82
8.81
8.81
8.15
8.14
7.76
3.76
3.75
3.74
3.72
3.71
3.70
3.69
3.58
2.60
2.07 Acetone
2.07 Acetone
2.07 Acetone
2.06 Acetone
2.06 Acetone
1.58
1.56
1.00
1.02
2.07
2.09
1.02
1.00
1.06
3.03
3.16
6.12
$^{1}$H chemical shift / ppm

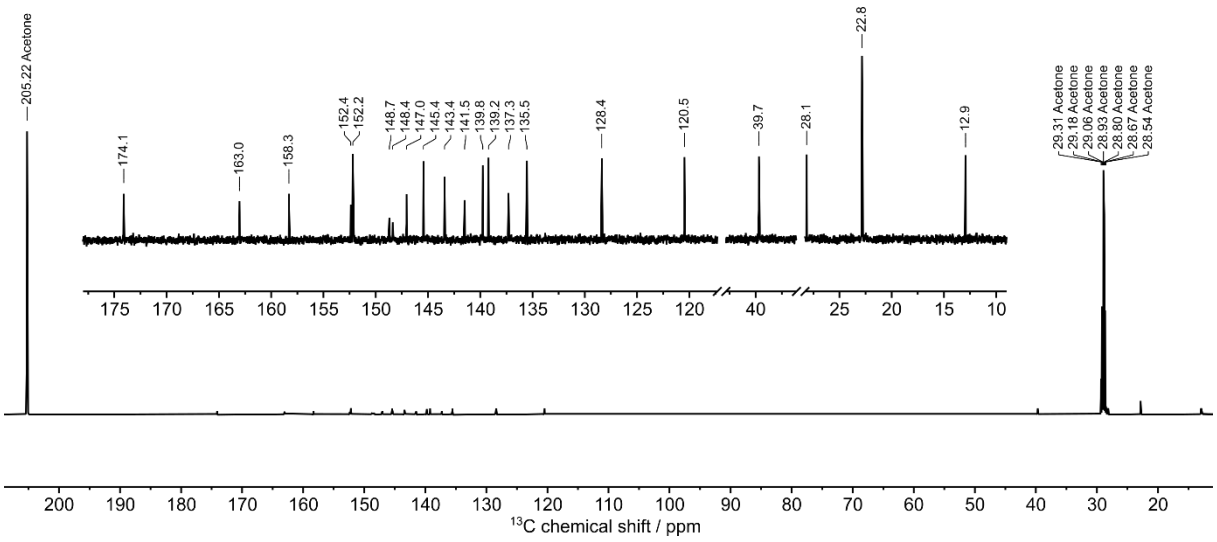
205.22 Acetone
174.1
163.0
158.3
152.4
152.2
148.7
148.4
147.0
145.4
143.4
141.5
139.8
139.2
137.3
135.5
128.4
120.5
39.7
28.1
22.8
12.9
29.31 Acetone
29.18 Acetone
29.06 Acetone
28.93 Acetone
28.80 Acetone
28.67 Acetone
28.54 Acetone
$^{13}$C chemical shift / ppm

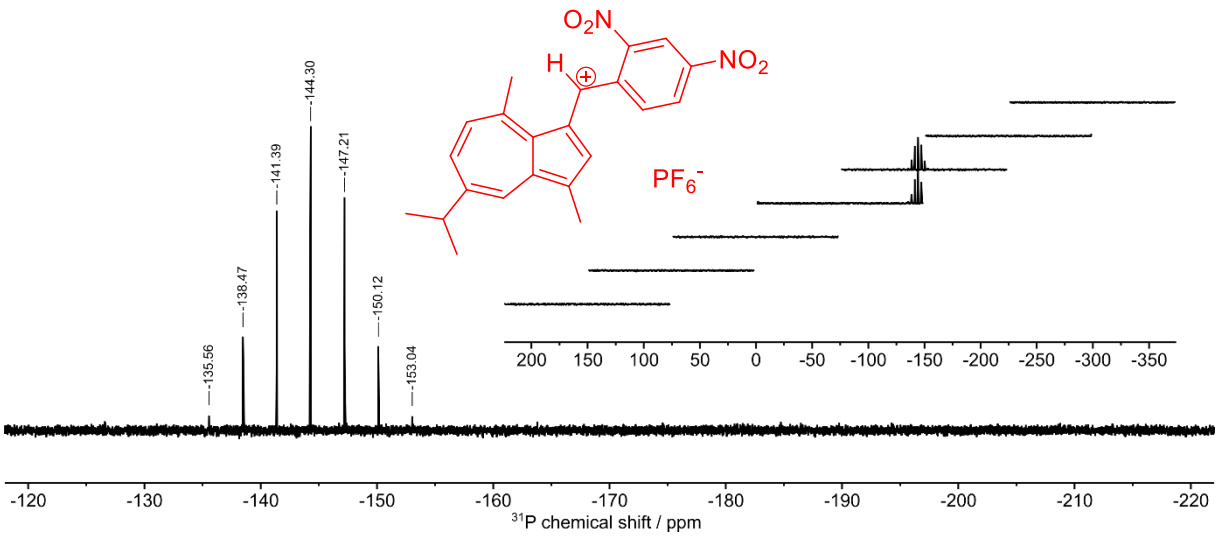
$O_2N$
H
$NO_2$
$PF_6^-$
-135.56
-138.47
-141.39
-144.30
-147.21
-150.12
-153.04
$^{31}$P chemical shift / ppm

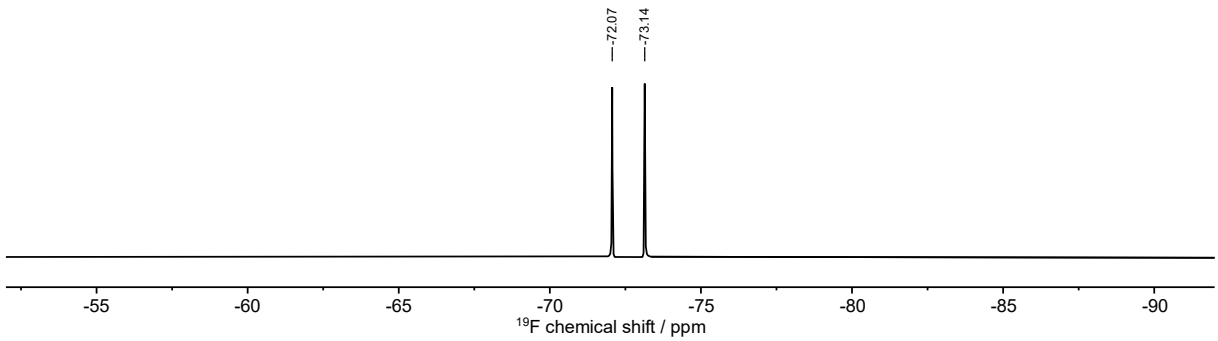
-72.07
-73.14
$^{19}$F chemical shift / ppm

**HR-ESI-MS** (positive ion mode):

Theory: 377.14958 [$M^+ = C_{22}H_{21}N_2O_4^+$]

Experimental: 377.14987 [$M^+$], $\Delta$ = 0.76 ppm

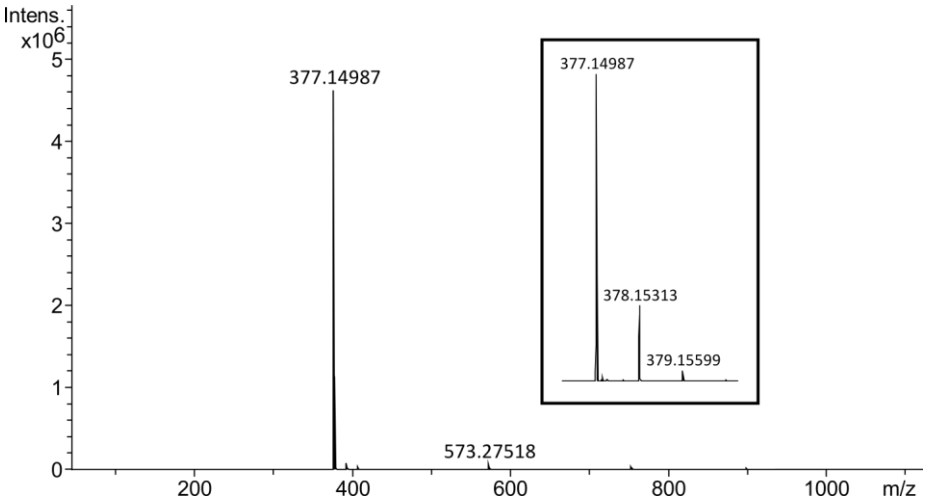


**HR-ESI-MS** (negative ion mode):

Theory: m/z = 144.96473 [$PF_6^-$]

Experimental: m/z = 144.96475 [$PF_6^-$], $\Delta$ = 0.16 ppm; 312.91846 [$P_3F_8O_4H_4^-$], $\Delta$ = -4.98 ppm

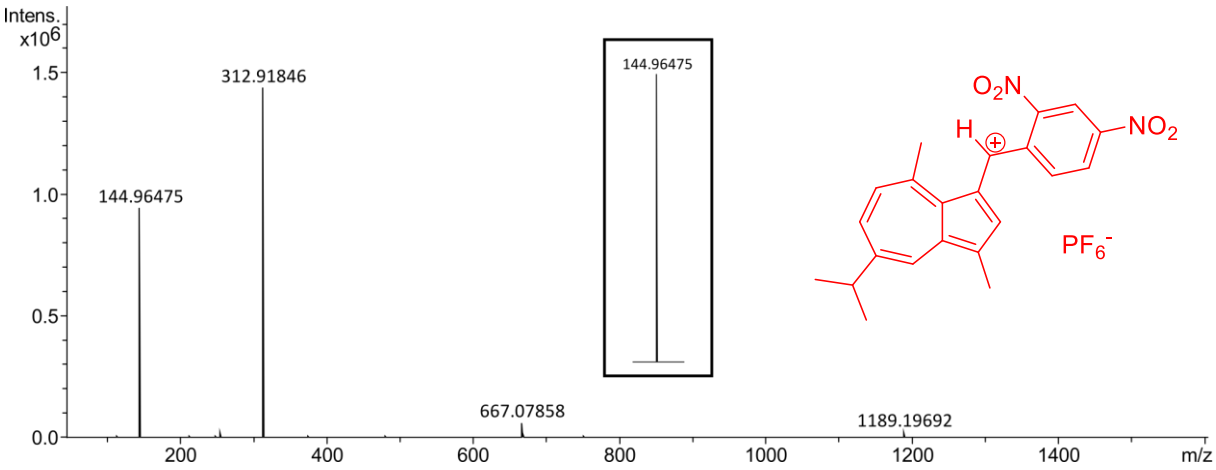


The HR-MS data (positive and negative ion mode) confirms the identity of cation and anion of **3** with a mass deviation of <1 ppm each. *m/z* = 312.91846 likely corresponds to an oligophosphate species. This is most likely formed in the MS ionisation process since the $^{31}P$ NMR spectrum shows $PF_6^-$ as the only phosphorous containing species (see above).

**ATR-IR:**

$\tilde{\nu}$ / cm$^{-1}$: 3108 (w, =C-H stretching), 2969–2875 (w, -C-H stretching), 1603 and 1527 (m, combined modes, aromatic system) 828 (vs, P-F asymm. stretching), 728 (m, P-F symm. stretching).[5]

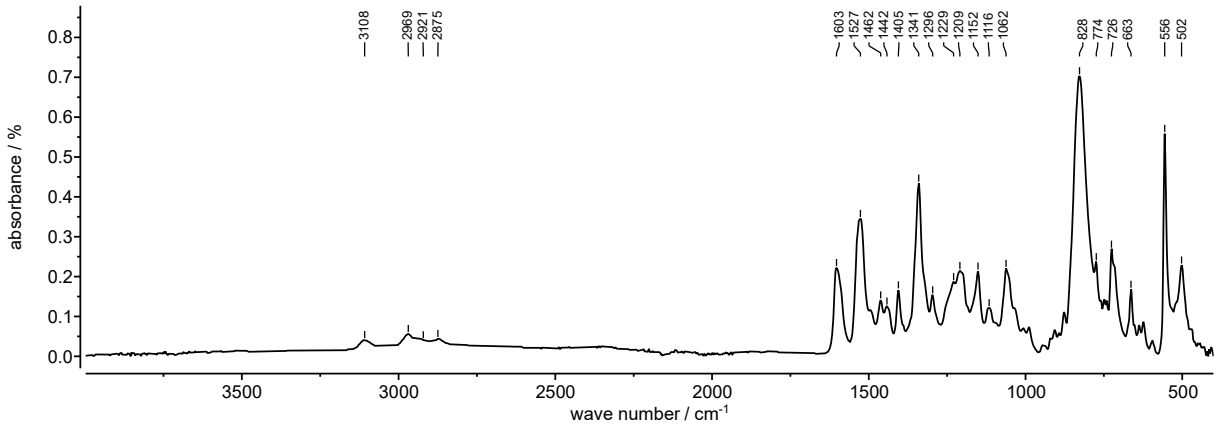


**UV/Vis:**

20.0 mg (38.3 µmol) of **3** were dissolved in 20 mL acetone (1.914 mmol/L) (for the UV/Vis spectrum see figure SI-6 left). From that, solutions with concentrations of 0.957, 0.383, 0.191, 0.077 mmol/L were created by dilution. The absorbance is plotted against the concentration, allowing for a linear fit (fig. SI-6 right) according to the LAMBERT BEER equation ($\varepsilon$: extinction coefficient in L mmol$^{-1}$ mm$^{-1}$, *A*: absorbance in a.u., *c*: concentration in mmol L$^{-1}$, *d*: path length in mm).

$$\varepsilon = \frac{\partial A}{\partial c} \cdot \frac{1}{d}$$

The resulting value for the extinction coefficient at 430 nm is $\varepsilon$ = 0.9332 L mmol$^{-1}$ mm$^{-1}$.

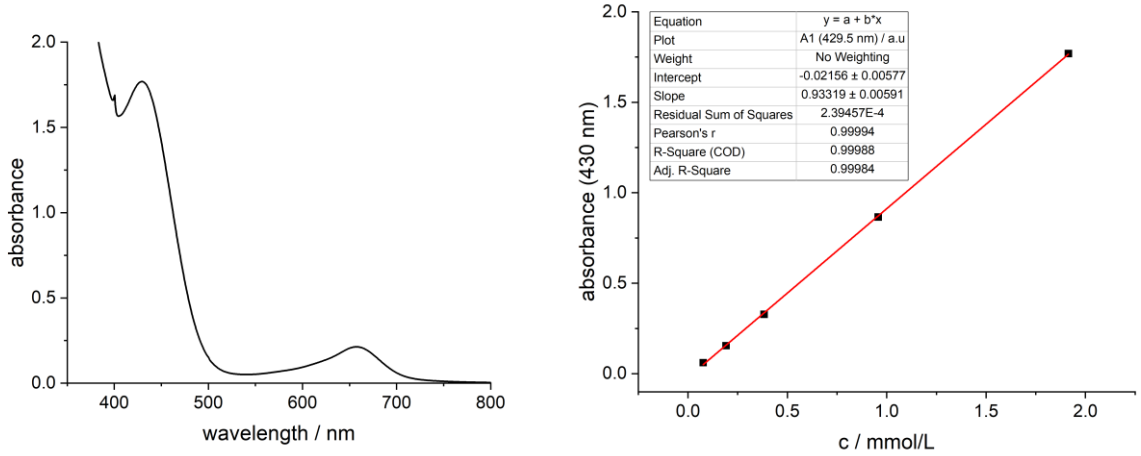


**Figure SI-6** Left: UV/Vis spectrum of species **3**. Right: Linear fit for the determination of the extinction coefficient of species **3**.

## 8. Identification and NMR characterisation of 4

When first monitoring the reaction of **1** and **2**, we were not aware that the cation **3** could react further. At room temperature, broadened signals were observed. We hypothesised that the broadening might be caused by hindered bond rotation in a thus far unknow species. To confirm this, we started reaction monitoring and, at a point where significant amounts of the additional signal set were formed, recorded spectra at significantly lower temperatures to stop the reaction from progressing. Additionally, we observed narrower signals at lower temperatures (see fig. SI-7 for $^1$H NMR spectra at temperatures between 320 and 260 K). This supported our hypothesis, that hindered bond rotation is present in the thus far unknown species.

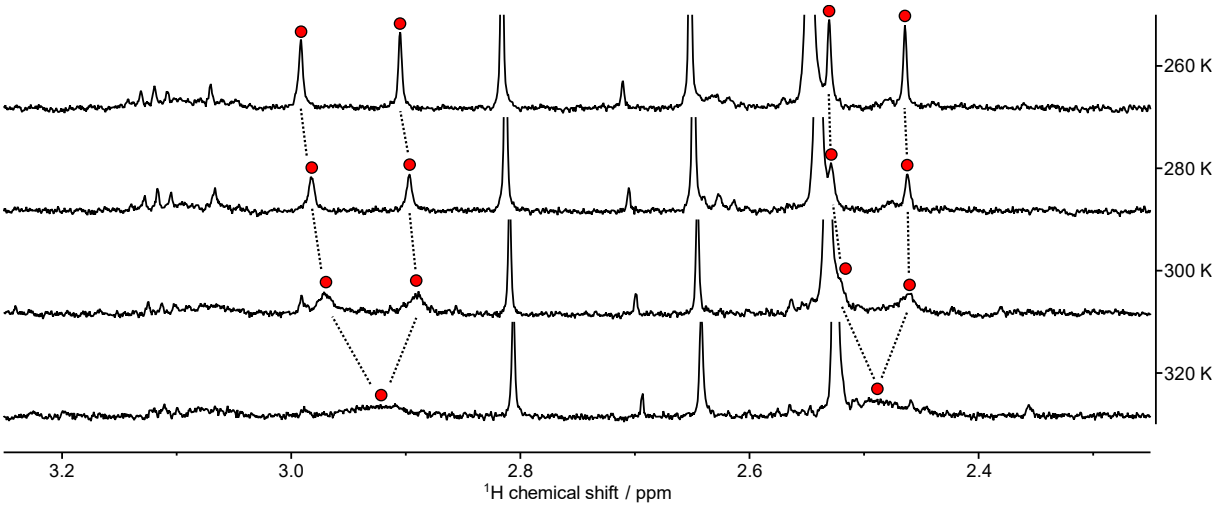


**Figure SI-7** Temperature series for a reaction mixture of **1**, **2**, and $HPF_6$ in THF-$d_8$ (sample no. kh03-039-B, **1**:**2**:$HPF_6$ = 2.1:3.4:54.2 mmol/L). The reaction was conducted at 300 K for 70 minutes to allow for a significant amount of **4** to form. Then, $^1$H-NMR spectra were recorded at temperatures between 260 K and 325 K.

We characterised the unknown species at 250 K. At this temperature, we were able to stabilise it and assign the signals to the bis-azulenyl species **4**. The formation of **4** from **3** and **1** continued until **1** was depleted, even at low temperatures. We did a full signal assignment from 1D $^1$H and 2D NMR (COSY, HSQC, HMBC) spectra from the reaction mixture, by discarding signals of known species (**1**, **2**, **3**, solvents).
The formation of such a species is in accord with azulene literature. Also, the occurrence of multiple rotamers, distinguishable by NMR, has literature precedence in the works of Ito.[6,7]

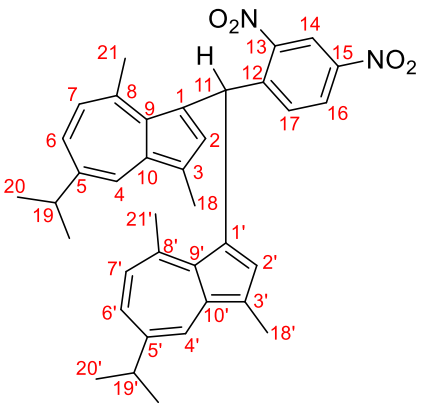


The following $^{1}$H and $^{13}$C NMR shifts are obtained from the reaction mixture at 250 K, as mentioned above. The $^{13}$C NMR chemical shifts are obtained from 2D (HSQC and HMBC) spectra, as it was not feasible to record a 1D $^{13}$C NMR spectrum with high enough S/N due to the low concentration of the sample. The two azulenyl substituents display different chemical shifts, which is attributed to them being diastereotopic due to the hindered bond rotation. This is reflected in atom numbering, where the atoms of the "second" substituent are labelled with a prime.

**$^{1}$H-NMR** (THF-$d_8$, 600 MHz, 250 K): $\delta$/ppm = 8.74 (d, $^{4}J_{H14\text{-}H16}$ = 2.4 Hz, 1H$_{14}$), 8.33 (s, 1H$_{11}$), 8.30 (dd, $^{3}J_{H16\text{-}H17}$ = 8.6 Hz, $^{4}J_{H16\text{-}H14}$ = 2.4 Hz, 1H$_{16}$), 8.21 (d, $^{4}J_{H4\text{-}H6}$ = 2.0 Hz, 1H$_4$), 8.17 (d, $^{4}J_{H4'\text{-}H6'}$ = 2.0 Hz, 1H$_{4'}$), 7.43 (dd, $^{3}J_{H6\text{-}H7}$ = 10.8 Hz, $^{4}J_{H6\text{-}H4}$ = 2.0 Hz, 1H$_6$), 7.36 (dd, $^{3}J_{H6'\text{-}H7'}$ = 10.5 Hz, $^{4}J_{H6'\text{-}H4'}$ = 2.0 Hz, 1H$_{6'}$), 7.03 (d, $^{3}J_{H17\text{-}H16}$ = 8.7 Hz, 1H$_{17}$), 6.98 (d, $^{3}J_{H7\text{-}H6}$ = 11.3 Hz, 1H$_7$), 6.88 (s, 1H$_{2'}$), 6.87 (d, $^{3}J_{H7'\text{-}H6'}$ = 12.0 Hz, 1H$_{7'}$), 6.85 (s, 1H$_2$), 3.09 (sept, $^{3}J_{H19\text{-}H20}$, 6.8 Hz, 1H$_{19}$), 3.06 (sept, $^{3}J_{H19'\text{-}H20'}$, 6.8 Hz, 1H$_{19'}$), 3.00 (s, 3H$_{21'}$), 2.91 (s, 3H$_{21}$), 2.53 (s, 3H$_{18'}$), 2.47 (s, 3H$_{18}$), 1.38 (d, $^{3}J_{H20\text{-}H19}$ = 6.7 Hz, 6H$_{20}$), 1.36 (d, $^{3}J_{H20'\text{-}H19'}$ = 6.7 Hz, 6H$_{20'}$).

**$^{13}$C-NMR** (THF-$d_8$, 150 MHz, 300 K): $\delta$/ppm = 149.2 (1C$_{12}$), 148.4 (1C$_{13}$), 146.4 (1C$_{15}$), 145.2 (1C$_{8'}$), 144.8 (1C$_8$), 141.4 (1C$_2$), 140.0 (1C$_5$), 139.7 (1C$_{5'}$), 139.0 (1C$_{2'}$), 138.4 (1C$_{10}$), 137.6 (1C$_{10'}$), 135.4 (1C$_6$), 135.4 (1C$_{6'}$), 134.2 (1C$_4$), 134.1 (1C$_{4'}$), 133.2 (1C$_{17}$), 133.0 (1C$_{9'}$), 131.7 (1C$_9$), 127.6 (1C$_1$), 127.5 (1C$_7$), 127.2 (1C$_{1'}$), 127.2 (1C$_{7'}$), 126.3 (1C$_{16}$), 124.5 (1C$_3$), 123.9 (1C$_{3'}$), 120.3 (1C$_{14}$), 42.5 (1C$_{11}$), 37.7 (1C$_{19}$), 37.6 (1C$_{19'}$), 26.3 (1C$_{21'}$), 26.1 (1C$_{21}$), 24.0 (2C$_{20}$), 23.9 (2C$_{20'}$), 12.2 (1C$_{18}$), 12.2 (1C$_{18'}$).

$^{1}$H NMR spectrum of the reaction mixture. Only the peaks of **4** are picked:

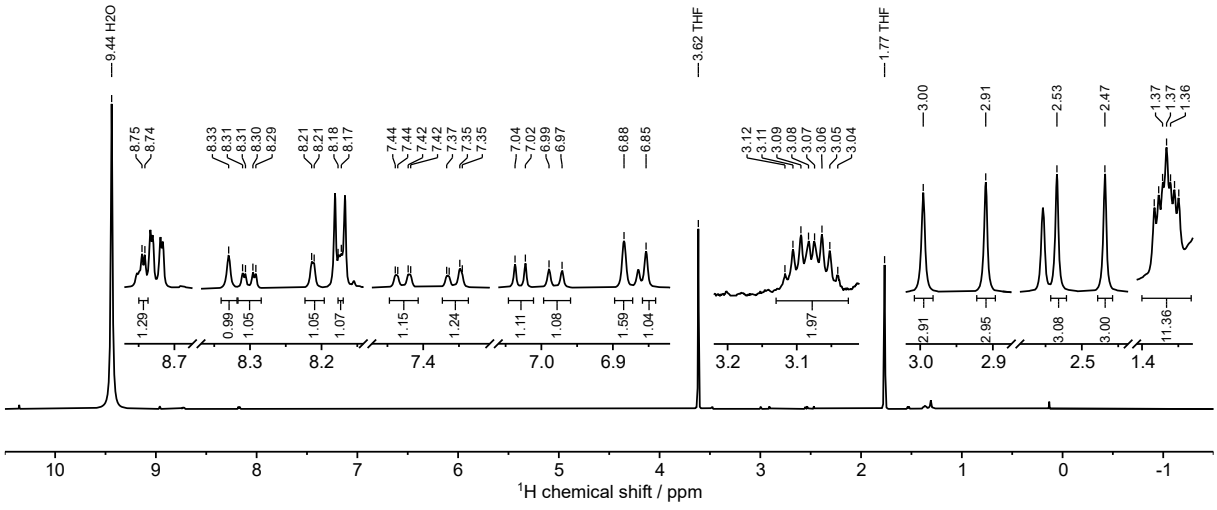

## 9. Identification and NMR characterisation of 1-H$^+$

Sample preparation (sample no. kh03-041): 8.2 mg guaiazulene **1** and 20 µL conc. $HPF_6$ (55 w% in $H_2O$) were dissolved in 650 µL of THF-$d_8$ in order to partially protonate **1**. On this sample, 1D and 2D NMR spectra were measured in order to determine the structure of **1-H$^+$** and assign signals.

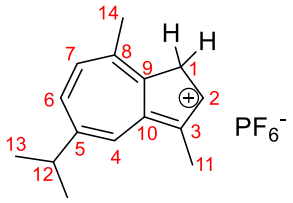


**$^1$H NMR** (THF-$d_8$, 600 MHz, 245 K): δ/ppm = 8.76 (s (br), 1H$_4$), 8.73 (s (br), 1H$_6$), 8.73 (s (br), 1H$_7$), 7.54 (m (br), 1H$_2$), 4.11 (m (br), 2H$_1$), 3.61 (sept, $^3J_{H12\text{-}H13}$ = 6.9 Hz, 1H$_{12}$) 3.03 (s, 3H$_{14}$), 2.46 (m (br), 3H$_{11}$), 1.48 (d, $^3J_{H12\text{-}H13}$ = 6.8 Hz , 6H$_{13}$).

**$^{13}$C NMR** (THF-$d_8$, 150 MHz, 245 K): δ/ppm = 172.9 (1C$_5$), 167.1 (1C$_9$), 166.3 (1C$_{10}$), 158.9 (1C$_8$), 149.3 (1C$_7$), 148.4 (1C$_2$), 145.6 (1C$_6$), 144.9 (1C$_3$), 139.7 (1C$_4$), 43.4 (1C$_1$), 39.7 (1C$_{12}$), 24.3 (1C$_{14}$), 22.9 (2C$_{13}$), 12.6 (1C$_{11}$).

$^1$H and $^{13}$C NMR spectra of the reaction mixture of guaiazulene **1** and protonated guaiazulene **1+H$^+$**. Only the peaks of **1+H$^+$** are picked.

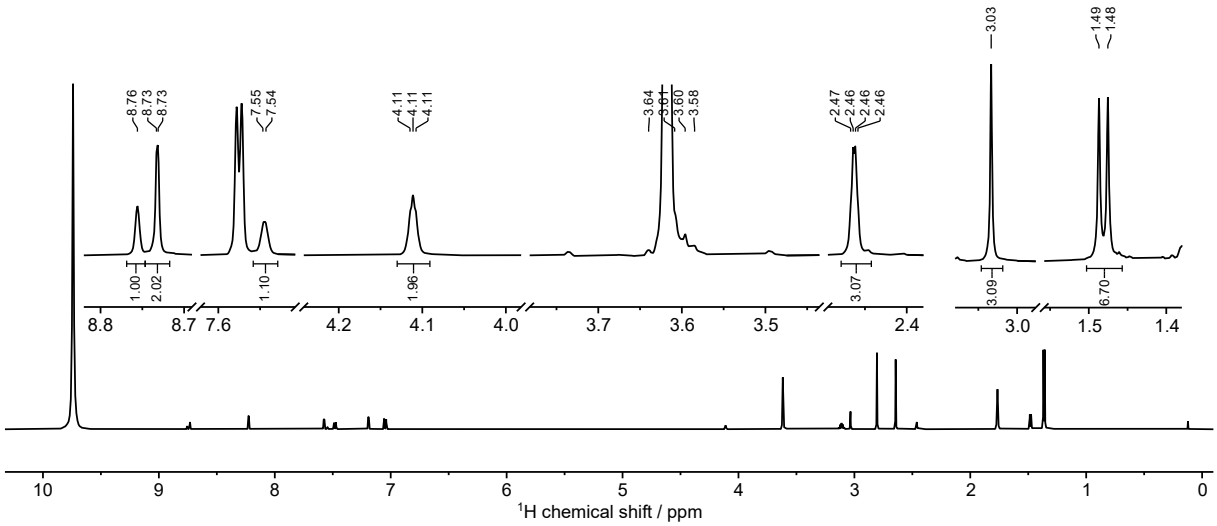


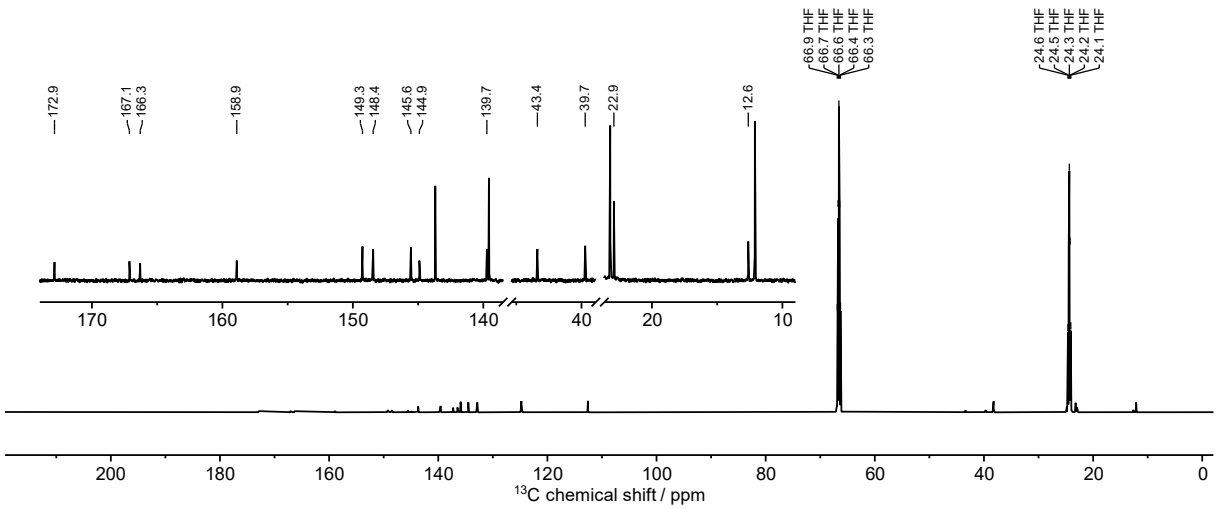

## 10. Detailed analysis of concentration profiles – variations of c($H^+$) and c(1)

As described in the main text, the acid catalysed reaction of guaiazulene and 2,4-dinitrobenzaldehyde **2** forms the cationic species **3** and the bis-substituted species **4** (see reaction scheme SI-1, repeated from main text).

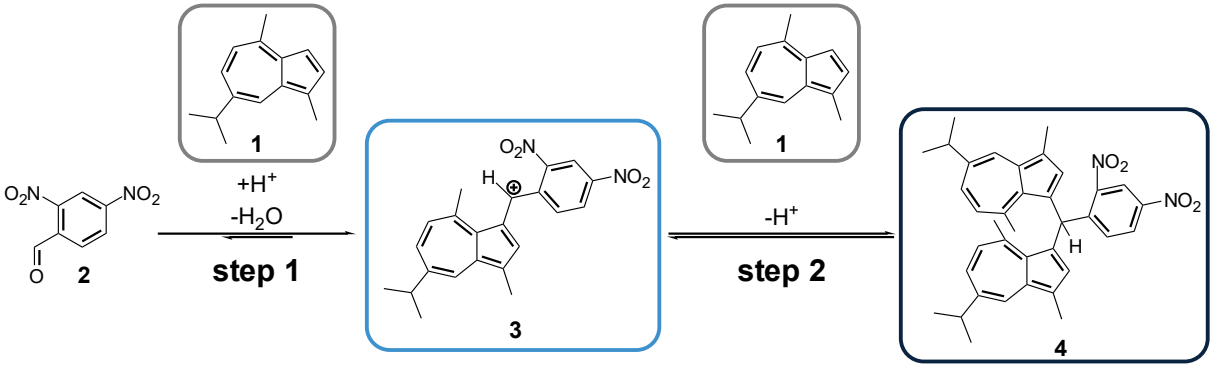


**Scheme SI-1** Simplified reaction scheme for the reaction of guaiazulene **1** and 2,4-dinitrobenzaldehyde **2**. This is repeated from the main text for clarity purposes.

While step 1 of the reaction consumes protons, step 2 releases them, making the outcome of the reaction very sensitive to the concentration of acid present in the reaction mixture. Additionally, the concentration of $PF_6^-$ might influence the reactivity of **3** through the formation of ion pairs,[8] which might also be influenced by the changing water content ($HPF_6$ is added as 55 wt.-% in water). At $c_0(HPF_6)$ = 108 mM, **3** is formed rapidly and almost no **4** is formed. At $c_0(HPF_6)$ = 20 mM, the concentration of **3** is negligible throughout the whole reaction and only **4** is observed. At $c_0(HPF_6)$ = 54 mM and $c_0(HPF_6)$ = 27 mM, the formation of **3** is observed, followed by the depletion of **3** and formation of **4**. The trend is displayed in figure SI-8. Additionally, a change in the speed of the reaction can be observed with changing $HPF_6$ concentration, with fast reactions at higher concentrations and slow reactions at lower concentrations.

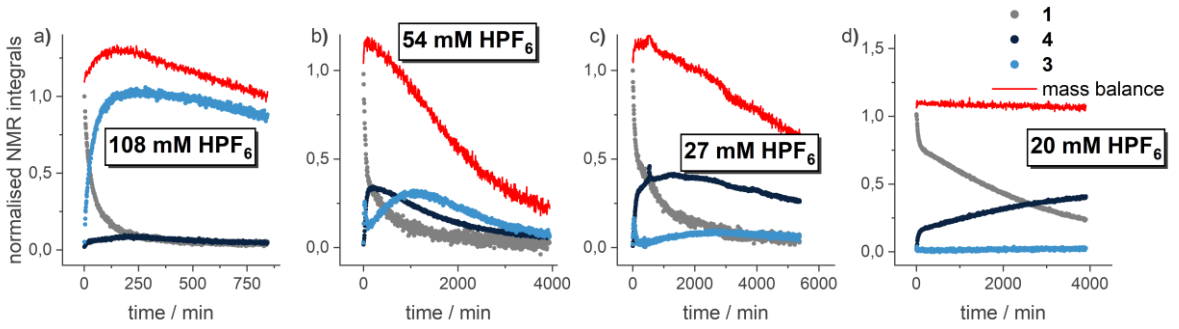


**Figure SI-8** Reaction monitoring at different concentrations of $HPF_6$ and otherwise identical initial conditions. With lowering acid concentration, the reaction gets slower and a higher relative concentration of **4** (dark blue) is observed. Mass balance ($I_{norm}$(**1**)+$I_{norm}$(**3**)+2*$I_{norm}$(**4**)) is given as a red line. The graphs a, b and d without mass balance are also displayed in the main text (Figure 3). Sample numbers: (a) kh03-053-B, (b) kh03-043-A, (c) kh03-054-B, (d) kh03-053-A. Sample compositions: **1**:**2**:$HPF_6$ = (a) 2.1:3.0:108 mmol/L, (b) 2.1:3.1:53.8 mmol/L, (c) 2.1:3.0:27.1 mmol/L, (d) 2.1:3.0:20.3 mmol/L.

The dependence on the $HPF_6$ concentration explains only part of the observed reaction profiles. Additionally, the equilibrium in step 2 depends on the concentration of **1** available at the respective time (limiting component). As **1** takes part in both reaction steps, the reaction system reacts dynamically to the concentration of **1**: At the beginning of the reaction, a large amount of **1** is available, so that it is consumed in both reaction steps, leading to the formation of **3** and subsequently **4**. **4** acts as a reservoir that slowly releases **1** and **3**, leading to another increase in c(**3**). This back-reaction is reinforced by the excess of **2**, which consumes the released **1**, forming additional **3**. If no decomposition would take place, a quasi-stationary state should be reached after the depletion of **2**, since then **1** participates only in the second reaction step. However, decomposition to unknown products does occur, therefore finally leading to the depletion of all species.

The mass balance (red lines in Figure SI-8) indicates that decomposition is taking place. The mass balance (given relative to guaiazulene units) is calculated as $I_{norm}$(**1**)+$I_{norm}$ (**3**)+2*$I_{norm}$ (**4**), where **4** is counted twice due to it containing two azulene units. Here, $I_{norm}$ is the normalised relative integral, which is directly proportional to the concentration of the compounds. The time courses observed for 54, 27 and 20 mM $HPF_6$ point at decomposition being faster at higher c($HPF_6$). Note, that for 108 mM $HPF_6$, the data is available for a shorter time window (750 instead of 4000 minutes), such that decomposition cannot be inferred from the mass balance, which is dominated by an initial rise. For all time courses, this initial rise in the mass balance is attributed to artifacts from signal integration due to overlap with small signals from unknown decomposition products or baseline distortion in crowded spectral regions. This effect causes an increase in the total integral but does not influence the shape of the concentration-time profiles.

When performing the reaction at an excess of guaiazulene **1** (more than 2:1 relative to dinitrobenzaldehyde **2**), a shift of the equilibrium towards **4** is expected. This would allow for **4** to be formed not as an intermediate but as the final reaction product. As can be seen in figure SI-9, this is indeed the case, further underpinning our interpretation of the reaction monitoring data.

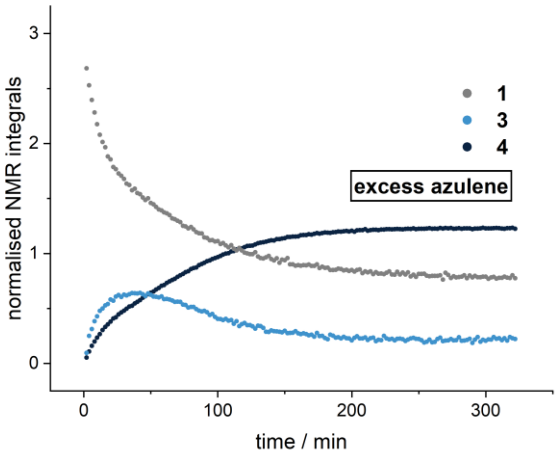


**Figure SI-9** Reaction monitoring at an excess of azulene (>2:1 with regard to **2**). Sample composition: **1**:**2**:$HPF_6$ = 8.6:3.1:54.2 mmol/L. Sample no.: kh03-040-A.

## 11. Proposed reaction mechanism

In order to expand the reaction scheme presented in the main text (scheme 2), we propose the reaction mechanism presented in scheme SI-2, which is in accordance with our observations and explains the formation of the species observed in the NMR spectra (**1**, **1+H⁺**, **2**, **3**, **4**). These are marked with boxes.

Step 1: The formation of **3** from **1** and **2**, which we labelled as reaction step 1, consists of multiple steps. First, 2,4-dinitrobenzaldehyde **2** is protonated, activating the carbonyl group for the nucleophilic attack of guaiazulene **1**. Subsequently, water is eliminated, forming **3**. The alcohol shown is not observed experimentally.

Step 2: Guaiazulene performs a nucleophilic attack at the bridging C-H group of the carbenium ion **3**, forming **4** after deprotonation.

Additionally, we observe NMR-spectroscopically, that guaiazulene **1** is in equilibrium with its protonated form **1+H⁺**.

Furthermore, decomposition is observed. A plausible pathway might start at compound **3**, as its positive charge makes it a likely candidate for further reactions. This is supported by reaction monitoring at low c($HPF_6$) (Figure SI-8d) or with excess **1** (Figure SI-9), which both feature low concentrations of **3** and high concentrations of **4**, and only little or no decomposition is observed. We interpret these observations to indicate decomposition starting at **3**. The occurrence of other decomposition pathways cannot be excluded.

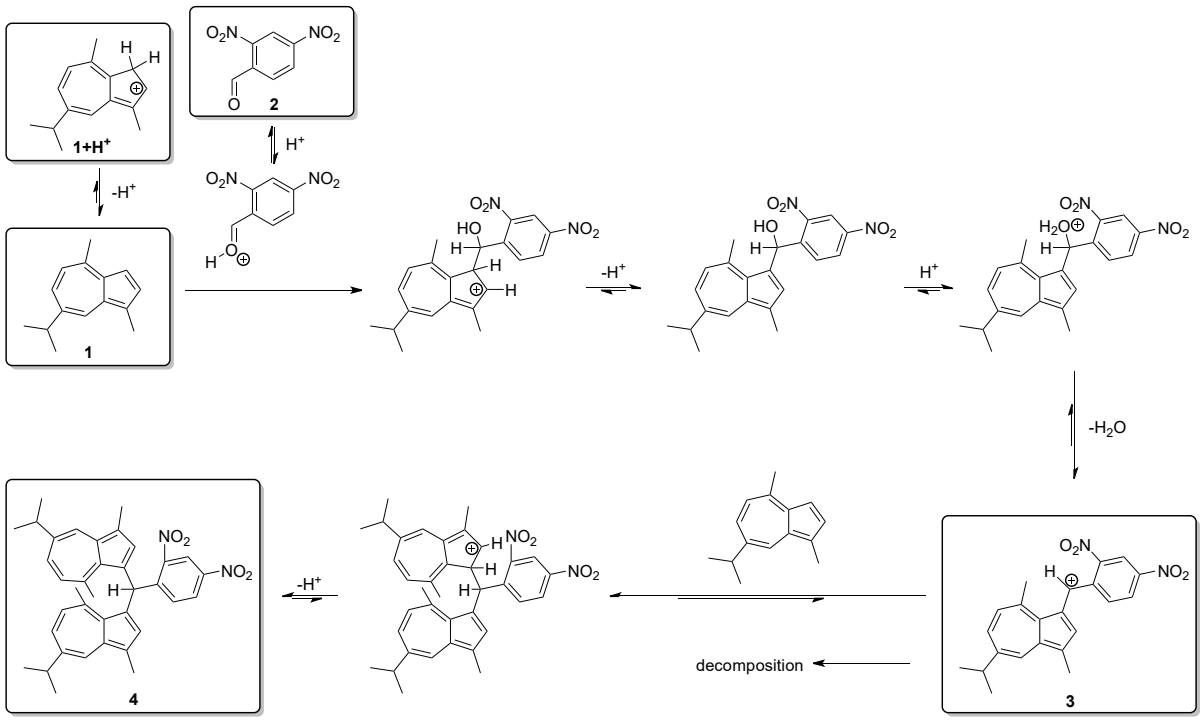


**Scheme SI-2** Proposed reaction mechanism for the reaction of guaiazulene **1** and 2,4-dinitrobenzaldehyde **2**.

## 12. Reaction kinetics simulation

In order to show that the proposed reaction scheme can produce a double maximum and therefore explain the observed intensity-time courses, a reaction kinetics simulation is performed using a simplified model of the reaction (see scheme SI-3).

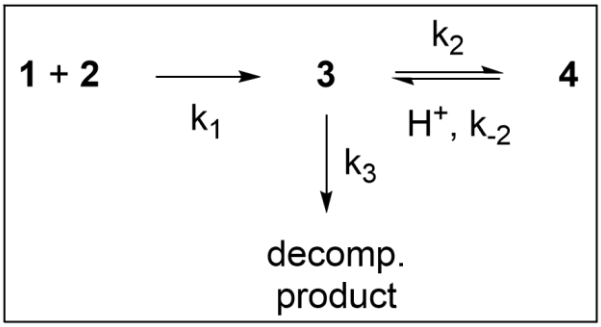


**Scheme SI-3** Simplified reaction scheme used for reaction kinetics simulation including the naming scheme for rate constants.

The following rate equations are used for the numerical simulation:

$dc(\mathbf{1})/dt = -k_1c(\mathbf{1})c(\mathbf{2}) -k_2c(\mathbf{1})c(\mathbf{3}) +k_{-2}c(\mathbf{4})c(H^+)$

$dc(\mathbf{2})/dt = -k_1c(\mathbf{1})c(\mathbf{2})$

$dc(\mathbf{3})/dt = +k_1c(\mathbf{1})c(\mathbf{2}) -k_2c(\mathbf{1})c(\mathbf{3}) +k_{-2}c(\mathbf{4})c(H^+) -k_3c(\mathbf{3})$

$dc(\mathbf{4})/dt = +k_2c(\mathbf{1})c(\mathbf{3}) -k_{-2}c(\mathbf{4})c(H^+)$

The simulated intensity-time courses are given in Figure SI-10. The initial concentrations are set to values similar to the experimental ones ($c_0(\mathbf{1}) = 2$, $c_0(\underline{\mathbf{2}}) = 3$, $c(H^+) = 50$). The time step for numerical simulation was set to dt = 0.5. The rate constants are manually adjusted so that a double maximum is observed ($k_1 = 0.008$, $k_2 = 0.1$, $k_{-2} = 0.000002$, $k_3 = 0.00035$). Therefore, the simulation shows that, with the right rate constants, the reaction model can yield a double maximum in the intensity-time course.

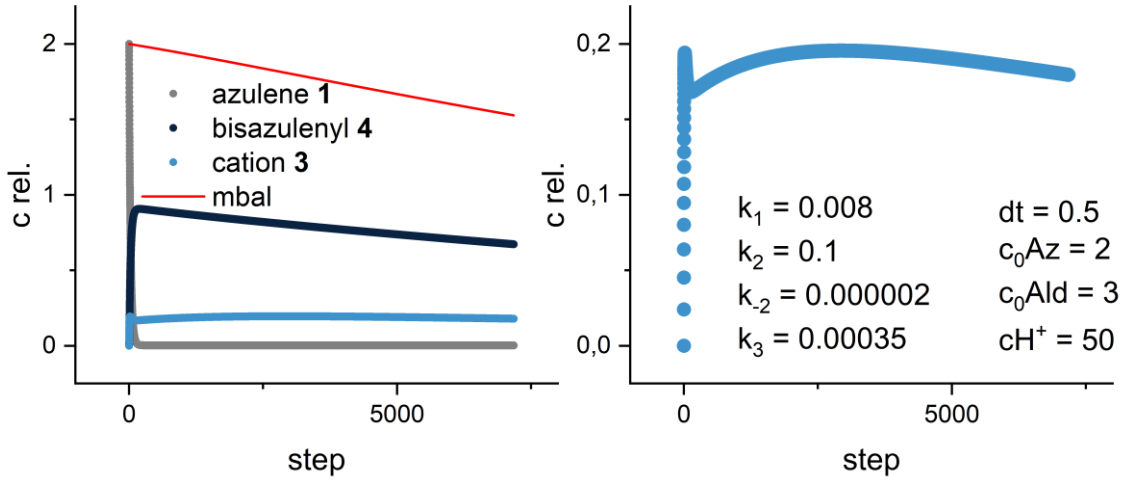


**Figure SI-10** Numerically simulated data according to the simplified reaction shown in Scheme SI-3. Left: Concentrations of compounds **1** (grey), **3** (light blue) and **4** (dark blue) and the mass balance (red line, c(**1**)+c(**3**)+2*c(**4**)). Right: Zoom for visual clarity, and values for initial concentrations and rate constants.

## 13. References


1 D. Herold, M. Brauser, J. Kind and C. M. Thiele, *Chem. – Eur. J.*, 2024, e202304016.
2 S. Takekuma, S. Hori, T. Minematsu and H. Takekuma, *Bulletin of the Chemical Society of Japan*, 2008, **81**, 1472–1484.
3 S. Takekuma, K. Sonoda, C. Fukuhara and T. Minematsu, *Tetrahedron*, 2007, **63**, 2472–2481.
4 Y. V. Kokunov, M. M. Ershova and G. A. Razgonyaeva, *Russ. J. Coord. Chem.*, 2002, **28**, 461–463.
5 D. S. Lakshmi, T. Cundari, E. Furia, A. Tagarelli, G. Fiorani, M. Carraro and A. Figoli, *Macromolecular Symposia*, 2015, **357**, 159–167.
6 S. Ito, N. Morita and T. Asao, *Bull. Chem. Soc. Jpn.*, 1995, **68**, 1409–1436.
7 S. Ito, N. Morita and T. Asao, *Chem. Lett.*, 1995, **24**, 475–476.
8 V. Burger, M. Franta, A. R. Ofial, R. M. Gschwind and H. Zipse, *J. Am. Chem. Soc.*, 2025, **147**, 5043–5050.